https://doi.org/10.5194/egusphere-2026-2333
Preprint. Discussion started: 8 July 2026

Bayesian-Informed Hybrid Deep Learning for GLOF Susceptibility and Hazard Escalation in the HKKH Region (2010-2020)

Farkhanda Abbas[a], Zhihua cai[b]

[a]School of Computer Science, China University of Geosciences, Wuhan 430074, China; shaminkhan0427@gmail.com

[b]School of Computer Science, China University of Geosciences, Wuhan 430074, China; zhcai@cug.edu.cn

*Correspondence: shaminkhan0427@gmail.com

Abstract. Rapid glacier retreat, complicated geography, and unpredictable weather make the Hindu Kush–Karakoram–Himalaya (HKKH) region extremely susceptible to Glacial Lake Outburst Floods (GLOFs). Current GLOF susceptibility assessments seldom take temporal dynamics or uncertainty into account, instead concentrating on either upstream lake conditions or downstream repercussions. An integrated, uncertainty-aware GLOF susceptibility framework that combines hybrid deep learning models with Bayesian probabilistic classification is presented in this paper. Spatiotemporal variations in glacial lakes and downstream terrain are captured using multi-temporal Landsat (2010–2016) and Sentinel-2 (2016–2020) imagery, SRTM DEM, Randolph Glacier & ICIMOD Inventory, morphological, hydrological, spatial, and topographical variables, and recorded GLOF events. CNN-LSTM, CNN-RNN, and Transformer-CNN models are trained using probabilistic labels produced by Bayesian inference. With AUC values between 0.90 and 0.92, the models demonstrate high predictive performance. High-altitude northern and central HKKH regions are becoming more vulnerable due to increased glacier melt, according to hazard escalation maps from 2010 to 2020. For regional GLOF risk assessment and disaster risk management, this framework offers a scalable tool.

1. Introduction

The greatest cryospheric system outside of the polar regions is found in the Hindu Kush–Karakoram–Himalaya (HKKH) region, which has over 70,000 glaciers. More than one billion people in South and Central Asia depend on it to meet their

https://doi.org/10.5194/egusphere-2026-2333
Preprint. Discussion started: 8 July 2026

water demands (Bolch et al., 2012; Kääb et al., 2018). This region is crucial for water security, agriculture, hydropower production, and ecosystem stability because it is the source of major river systems including the Indus, Ganges, and Brahmaputra. However, the likelihood of Glacial Lake Outburst Floods (GLOFs) has increased dramatically due to the acceleration of glacier retreat and the growth of glacial lakes caused by rising temperatures. These occurrences put infrastructure, transboundary water systems, and human lives at grave risk (Carrivick & Tweed, 2016; Shrestha & Aryal, 2011). GLOFs happen when natural dams, which are usually made of ice or unconsolidated moraine debris, abruptly collapse as a result of internal instability, excessive precipitation, ice avalanches, or seismic activity. Their catastrophic power is demonstrated by a number of historical occurrences throughout the HKKH region. For instance, hydroelectric infrastructure in Nepal was severely damaged by the Dig Tsho GLOF in 1985 (Vuichard & Zimmermann, 1987), whereas the Lugge Tsho incident in Bhutan in 1994 caused a considerable loss of lives and property (Richardson & Reynolds, 2000). Large-scale breakdowns have been reported throughout High Mountain Asia in more recent times (Shugar et al., 2021). When taken as a whole, these incidents highlight the critical necessity for extensive and methodical evaluations of GLOF susceptibility.

Due to the region's complicated geography, a lack of data, and the dynamic nature of glacier lake systems, it is still difficult to reliably identify GLOF-prone lakes despite a great deal of research. The ability of many susceptibility studies to depict temporal lake evolution, hazard escalation, and uncertainty in lake-failure processes is limited because they rely on static snapshots of lake and terrain parameters. The majority of study has concentrated on particular lakes or short-term observations, and comprehensive, large-scale spatiotemporal assessments are still scarce. Prior studies have documented previous GLOFs and identified their tiggers (Allen et al., 2022; Mir et al., 2025; Rinzin et al., 2021; Zheng et al., 2021). Specifically, there are few integrated studies that evaluate glacial lake evolution and potential flood risk over decadal timeframes by combining hydrological and geomorphological factors with remote sensing-based lake boundary extraction. Furthermore, because spectral distinction is difficult, ice-covered lake dynamics are frequently disregarded, which leaves predictions of lake expansion and related risks questionable (Bolch et al., 2012; Ye et al., 2024).

Determining the boundaries of glacial lakes and monitoring changes in lake size and volume over time have shown to be successful uses of remote sensing methods, especially the Normalized Difference Water Index (NDWI). Originally presented by (McFeeters, 1996) to map water bodies, it has effectively captured the growth of glacier lakes in the Everest region (Shea

https://doi.org/10.5194/egusphere-2026-2333
Preprint. Discussion started: 8 July 2026

et al., 2015), measured changes over several decades in High Mountain Asia (Nie et al., 2017), and monitored both ice-free and partially ice-covered lakes in the Himalayas (Zhou et al., 2024). Key lake parameters, such as lake area, volume, and ice-free extent, can be extracted using multi-temporal NDWI analysis. These parameters can then be combined with spatial variables, such as proximity to glaciers, upstream watershed and glacier area, slope, topographic potential, downstream slope, and floodplain area. It is also possible to include indicators of dam stability and failure potential, such as excess volume and Propagation Probability Index (IPP) breach volume. A solid foundation for computing posterior probability and categorizing lakes as GLOF-prone or non-GLOF is provided by this integrated technique. Regional mapping of glacial lakes and morphometric characteristics using satellite imagery and DEMs has been made possible by developments in remote sensing and GIS (Nurakynov et al., 2025; Pandey et al., 2016; Ye et al., 2024). Multi-criteria decision-making methods such as AHP and fuzzy logic have been widely applied to rank GLOF susceptibility (Das & Sharma, 2024). More recently, machine learning and deep learning models have demonstrated improved predictive performance by capturing non-linear relationships among hazard indicators (Pourghasemi et al., 2020; Rahmati et al., 2019). Nevertheless, a lot of machine learning-based research still relies on binary or deterministic labels from past inventories, which fail to appropriately represent contextual interdependence and ambiguity in GLOF processes. GLOF probability or return periods have been estimated using Bayesian statistical techniques (Fischer et al., 2021; Vogel et al., 2024), However, these techniques are frequently used without deep learning and are restricted to upstream susceptibility; they do not take use of downstream system characteristics or spatiotemporal satellite observations.

To address these limitations, this study introduces a Bayesian deep learning framework that integrates probabilistic reasoning with hybrid neural network architectures. Multi-temporal Landsat imagery (2010–2016) and Sentinel-2 imagery (2016–2020) are used to capture temporal variations in lake area and volume, while DEM-derived terrain variables, glacier inventories, and hydrological indicators characterize spatial controls on GLOF susceptibility. Bayesian inference is employed to generate uncertainty-aware susceptibility soft labels, which are subsequently used to train CNN–LSTM, CNN–RNN, Transformer–CNN, and Hybrid Neural Network (HNN) models. The particular goals of this research are to:

- Using multi-source remote sensing and geographic data, create a temporally informed GLOF susceptibility dataset for the HKKH region;

https://doi.org/10.5194/egusphere-2026-2333
Preprint. Discussion started: 8 July 2026

- Use probabilistic labels to assess how well hybrid deep learning models perform under spatial cross-validation;
- Examine important hydrological and spatial factors that affect GLOF susceptibility; and
- Chart the spatiotemporal trends of GLOF risk escalation in the HKKH region between 2010 and 2020.
- This study's main goal is to develop a scalable, uncertainty-aware large-scale GLOF susceptibility assessment framework that enhances hazard prediction and aids early warning systems, climate adaptation planning, and catastrophe risk reduction in extremely exposed areas like HKKH.

2. Material & methods

2.1 Study area

Afghanistan, Pakistan, India, Nepal, Bhutan, China, and Myanmar are all included in the HKKH region. The largest cryospheric mass outside of the polar zones, it is home to more than 70,000 glaciers and supplies water to major rivers like the Ganges, Brahmaputra, and Indus, supporting ecosystems, hydropower, agriculture, and water security. The area is particularly vulnerable to GLOFs due to its steep topography, quick glacier retreat, and unpredictable climate (Figure 1).

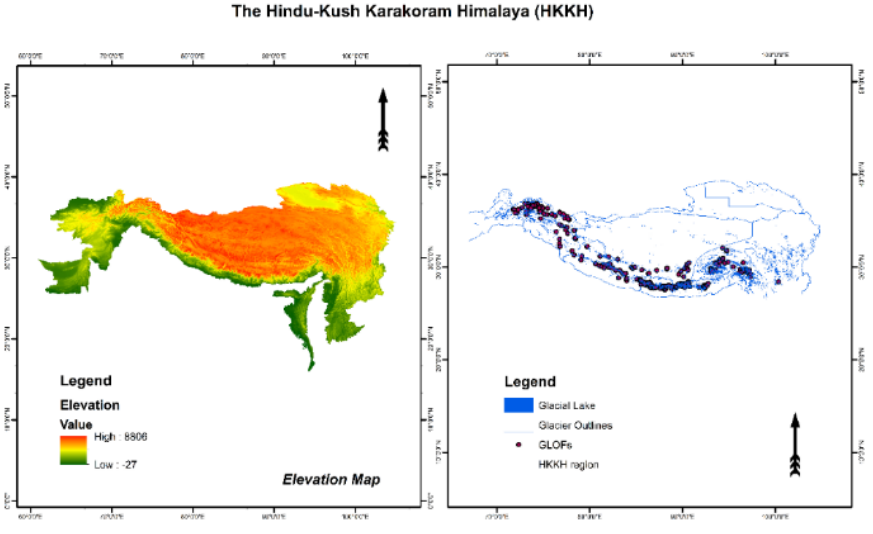

Figure 1. Shows the outline of the HKKH region as well as the historical GLOFs recorded in the region with Elevation Map.

https://doi.org/10.5194/egusphere-2026-2333
Preprint. Discussion started: 8 July 2026

2.2 Methodology

In order to categorize glacier lakes according to their tendency for outburst floods, the methodology used to evaluate GLOF susceptibility in the HKKH region incorporates remote sensing data, Bayesian modeling, and geomorphic analysis. In order to minimize cloud and snow contamination and capture seasonal variability in glacial lake extent, Sentinel-2 imagery from 2016–2020 and Landsat imagery from 2010–2016 were chosen for the analysis of glacial lakes in the HKKH region, concentrating on the pre-monsoon (March–May) and post-monsoon (September–November) months. The Normalized Difference Water Index (NDWI) threshold of >0.3 was used to define water bodies, in accordance with accepted techniques for recognizing turbid, high-altitude lakes (Hu et al., 2022; McFeeters, 1996). Since maximum and minimum composites produced less consistent findings, a median composite strategy was employed to reduce noise from clouds, snow, and seasonal anomalies (Jensen, 2009). A minimal area threshold of 0.002 km² (about three Landsat pixels) was used to rule out small or transient ponds that are unlikely to cause GLOFs (Xu, 2006). The standard deviation throughout the multi-temporal composite was used to quantify lake area uncertainty, and slope and elevation masks were used to reduce residual misclassification caused by snow, ice, or cloud aberrations (Huss et al., 2017). In order to provide soft labels for training, the resulting dataset which included 23,000 glacial lakes connected with glaciers were further processed using hydro-morphologic and geomorphic parameters (such as lake area, volume, proximity to glaciers, and upstream watershed) (Table 1). Thresholds (Table 2) for important parameters were combined with prior weights that indicate their relative relevance to create the Bayesian soft labels. The posterior probability of each lake being GLOF-prone were then determined using the Bayesian model, which integrated the contributions of several lake attributes as well as the uncertainty of the data. A more adaptable and trustworthy evaluation of GLOF susceptibility was made possible by this probabilistic classification method. Two subsets of the dataset were created: a hold-out test set and a training set. In order to prevent circularity, 900 lakes with documented GLOFs were excluded from the training set, which was labelled using a Bayesian framework(Beven & Binley, 1992). GLOF-prone lakes (n = 675) were defined as having posterior probabilities greater than 0.7, while non-GLOF lakes (n = 225) had probabilities less than 0.7. Nine hundred lakes with confirmed past GLOFs made up the hold-out test set, which was set aside for independent validation of the model's performance, sensitivity to threshold changes, and forecast dependability (Pathak et al., 2025). This guaranteed that the testing represented actual GLOF events and the training depended on Bayesian labelling, offering an objective evaluation

https://doi.org/10.5194/egusphere-2026-2333
Preprint. Discussion started: 8 July 2026

of the resilience of the model. Soft labels from the basin dataset were used for training, and the GLOF historical inventory was used as an independent test set to assess the model's performance. A combination of topography, glaciological, and historical factors with particular threshold criteria is used to identify non-GLOF lakes (Khadka et al., 2021). From SRTM DEM, stable conditions are indicated by lakes with a dam slope of less than 15°, an upstream watershed area of less than 5 km², A potential flood volume of less than 1 million m³, a breach volume of less than 0.5 million m³, and a low connection index (<0.3). As per glacial lake outlines, lakes with gentle dam slopes (<15°), a lake area of less than 0.1 km², and a lake volume of less than 0.05 million m³ are less likely to fail based on these criteria we selected 225 lake as potential non-GLOF candidate (Table 2) which was further verified with Bayesian probability index (Table 3) then the trained model was applied to the entire dataset of 23,000 lakes to generate GLOF susceptibility predictions across HKKH. The reliability of the methodology for identifying GLOF-prone lakes in the HKKH region was ensured by cross-validating the final classification results with historical GLOF records (Figure 2).

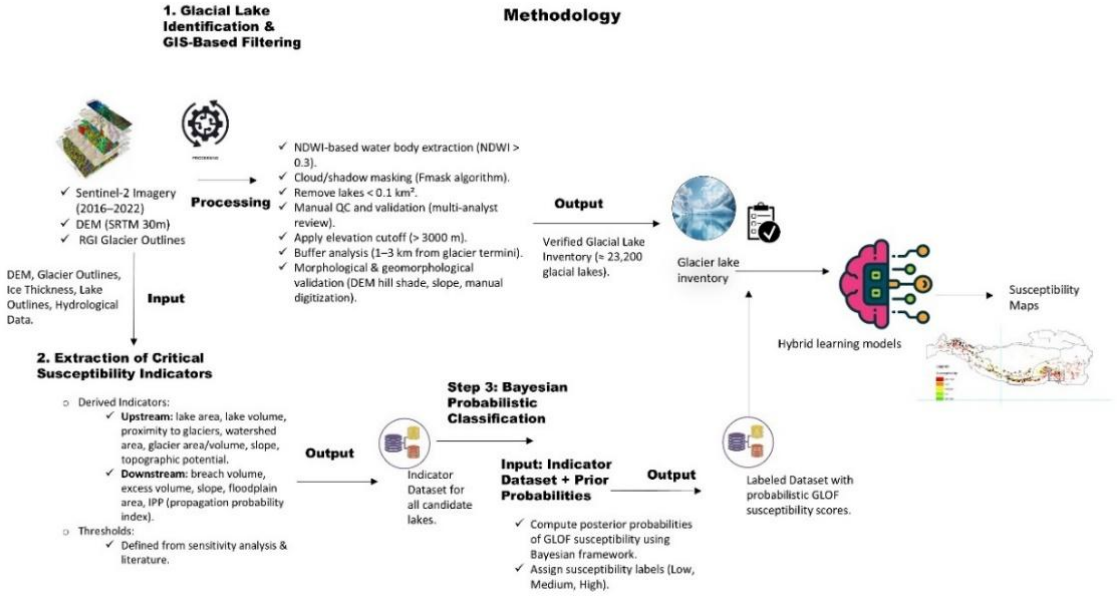

Figure 2. Shows the structure of process driven GLOF indicator system, geospatial database, Bayesian classification with hybrid models and their integration for susceptibility mapping.

https://doi.org/10.5194/egusphere-2026-2333
Preprint. Discussion started: 8 July 2026

Table 1. Data sources and spatial resolutions of datasets used for extracting indicators related to glacial lakes, glaciers, and topographic features in the GLOF hazard assessment.

Data	Indicator	Source	Scale/Resolution
SRTM Digital Elevation Model (DEM)	Topographic potential, upstream watershed area, dam slope, potential flood volume, breach volume, excess volume, propagation probability index, index of connectivity	USGS	30 m
Glacier outlines	Upstream glacier area	The Randolph Glacier Inventory 6.0 data (RGI-Consortium, 2017) is available at RGI	30 m
Glacial lake outlines	Glacial lake area, glacial lake volume, dam slope, potential flood volume, breach volume	Glacial lake inventory in 2015 (Zheng et al., 2021) is available at Zenodo	30 m
Glacier ice thickness	Upstream glacier volume	The composite glacier ice thickness data (Farinotti et al., 2019) is available at ETH Zurich	15 m
Glacier lake points	Specific locations of glacier lake outburst events	Glacier lake points ICIMOD is available at ICIMOD and Global Glacial Lake Inventory: 2015. Available at Zenodo	30 m
Landsat imagery (2010–2016)	Glacial lake detection, lake area, lake volume	USGS (United States Geological Survey)	30 m
Sentinel-2 imagery (2016-2020)	Glacial lake detection, lake area, lake volume	European Space Agency (ESA)	10m

Table 2. Presents the threshold values for various parameters used in both upstream and downstream areas, which were derived from sensitivity studies.

Parameter	Threshold (Upstream)	Threshold (Downstream)	Sensitivity Study Results: Accuracy (%)
Lake Area	> 0.1 km² (Larger lakes more likely to be dammed or unstable)	-	70% to 85%

https://doi.org/10.5194/egusphere-2026-2333
Preprint. Discussion started: 8 July 2026

Lake Volume	> 20 million m³ (Larger lakes have higher potential for catastrophic outbursts)	-	75% to 90%
Proximity to Glacier	< 2 km (Lakes closer to glaciers are more likely to be impacted by glacial retreat or instability)	-	80% to 90%
Upstream Watershed Area	> 50 km² (Larger upstream watershed areas contribute to higher potential flood volume)	-	70% to 85%
Upstream Glacier Area	> 3 km² (Larger glaciers have more significant impact on lake dynamics and outburst risks)	-	75% to 90%
Slope (Upstream Terrain)	> 30° (Steep slopes increase risk of instability, landslides, and sudden outbursts)	-	70% to 80%
Topographic Potential	High (High topographic potential indicates areas where lakes could be dammed by unstable moraines or glaciers)	-	75% to 85%
Upstream Glacier Volume	> 50 million m³ (Larger glaciers produce more meltwater, leading to higher GLOF risk)	-	80% to 90%
Excess Volume (Downstream)	-	> 50,000 m³ (Higher excess volume of unstable material, increasing GLOF impact)	75% to 90%
Propagation Probability Index (IPP)	-	High (Strong connectivity between lake and downstream flood pathways)	80% to 95%
Breach Volume (Downstream)	-	> 500,000 m³ (Larger breach volumes lead to more severe GLOF impacts)	80% to 90%
Downstream Slope	-	> 30° (Steep downstream slopes increase the velocity of floodwaters)	70% to 85%
Floodplain Area (Downstream)	-	Large (Floodplain areas downstream allow for extensive water spread)	75% to 85%

2.3 model description and hyperparameter setting

The input feature space is not entirely static, even if a number of topography and geomorphic factors (such as slope, elevation, and valley constriction) are treated as time-invariant during the study period. Interannual changes in lake area and spatial arrangement are captured by multi-temporal lake extent measures generated from Landsat (2010–2016) and Sentinel-2 (2016–2020) images. While static landscape variables were repeated over time steps, these temporally changing features were integrated as sequential inputs. In this context, multi-year patterns in lake evolution and spatial context were aggregated using recurrent (LSTM/RNN) and attention-based components instead of modelling physical time-dependent triggering processes. Therefore, rather than being predictors of dynamic lake failure mechanisms, the temporal modules serve as sequence-aware

https://doi.org/10.5194/egusphere-2026-2333
Preprint. Discussion started: 8 July 2026

feature integrators. While recognizing that the underlying covariates do not fully represent dynamic process factors, this design decision attempts to portray stable spatial configurations and progressive lake extension tendencies. The optimal configurations for each model component (CNN, LSTM, RNN, Transformer) were chosen using both grid search and manual tuning (Table 3) (Kernbach & Staartjes, 2021; Wang et al., 2022). Integration strategies for spatial and temporal features were evaluated for predictive accuracy, with final configurations chosen based on AUC-ROC, overall accuracy, and stability across cross-validation folds.

Table 3. Model architectures, components, hyperparameters, and combination strategies for hybrid deep learning models integrating CNNs with LSTMs, RNNs, and Transformers.

Model	Component	Feature Type	Hyperparameters	Combination Strategy
CNN-LSTM Hybrid	CNN	Static	Layers: 3–5; Filters: 32–128; Pooling: 2×2/3×3; ReLU; Dropout: 0.2–0.5	Extract static features, aggregate, concatenate with LSTM output
	LSTM	Temporal	Units: 50–200; Layers: 1–3; Dropout: 0.2–0.5; Activation: tanh/ReLU	Sequence-aware feature integration from multi-year lake metrics
CNN-RNN Hybrid	CNN	Static	Same as CNN-LSTM	Extract static features, aggregate, concatenate with RNN output
	RNN	Temporal	Units: 50–200; Layers: 1–3; Dropout: 0.2–0.5; Activation: tanh/ReLU	Sequence-aware integration of temporal lake features
Hybrid Neural Network (HNN)	CNN / LSTM / RNN	Static + Temporal	Same as CNN-LSTM & RNN	Feature fusion from static + temporal modules, final dense classifier
Transformer-CNN	CNN	Static	Same as CNN-LSTM	CNN extracts spatial features
	Transformer	Temporal	Attention heads: 4–12; Layers: 2–6; Hidden: 256–1024; FFN: 512–2048	Model feature interdependencies, integrate with CNN output

2.4 Bayesian Classification for GLOF susceptibility

Glacial lakes were classified as either GLOF prone or non-GLOF prone using a Bayesian probabilistic classification framework. Because of the low base rate of recorded outburst episodes in the HKKH, previous probabilities were based not only on historical inventory like the High Mountain Asia GLOF dataset and ICIMOD records but also on expert opinion based thresholds *(Fischer et al., 2024; Veh et al., 2020)*. In order to produce uncertainty-aware labels for further model training,

https://doi.org/10.5194/egusphere-2026-2333
Preprint. Discussion started: 8 July 2026

posterior probabilities were calculated using Bayes' theorem from important hydro morphologic and geomorphic parameters, such as lake area, volume, proximity to glaciers, and watershed characteristics:

$$P(Class|Features) \propto (P(Class) \prod_i P(Feature_i|Class)$$

Where ($P(Class)$ is Prior probability of GLOF or Non-GLOF, $P(Feature_i|Class)$ is Likelihood of observing feature i given the class, Posterior is probability of class given the features Continuous feature likelihoods were modelled as Gaussian distributions:

$$P(x|C) = \frac{1}{\sqrt{2\pi\sigma_C^2}} \boldsymbol{exp}\left(-\frac{(x-\mu C)^2}{2\sigma_C^2}\right)$$

Where $\boldsymbol{\mu C}$ and , $\boldsymbol{\sigma_C^2}$ are the mean and variance of the feature within class C. Naïve Bayes approach combined continuous (e.g., lake area, volume) and categorical (e.g., topographic potential, IPP) variables (Table 4). Beta distributions were used to model class priors π~ Beta(a,b), with parameters a and b encoding expected proportions of GLOF-prone lakes based on historical rates (e.g., weak priors Beta(1,1) or strong priors Beta(3,97)). Posterior class probabilities were computed as:

$$\mathrm{E}[\pi \mid data] = \frac{a + n_1}{a + b + n_1 + n_0}$$

where n_1 and n_0 are counts of GLOF-prone and non-GLOF lakes in the observed data, respectively. Spatially varying priors π_r were considered to account for sub-basin differences in occurrence rates (Veh et al., 2020). Lakes were classified as GLOF prone using posterior probabilities above the susceptibility threshold (e.g., 0.7), resulting in high-quality soft labels for hybrid deep learning model training. Instead of using strict binary criteria, this probabilistic labelling allows models to learn nuanced spatial and contextual susceptibility patterns by capturing uncertainty and contextual dependencies (Table 4) (Table 5) (Li et al., 2024; Nguyen et al., 2014).

https://doi.org/10.5194/egusphere-2026-2333
Preprint. Discussion started: 8 July 2026

Table 4. Sample glacial lakes with key susceptibility indicators, posterior probabilities, and final Bayesian classification.

Lake ID	Lake Area (km²)	Lake Volume (million m³)	Proximity to Glacier (km)	Upstream Watershed Area (km²)	Upstream Glacier Area (km²)	Slope (°)	Topographic Potential	Upstream Glacier Volume (million m³)	Excess Volume (m³)	IPP	Breach Volume (m³)	Downstream Slope (°)	Floodplain Area (km²)	Posterior Probability	Classification
1	6.0	25.0	1.5	60.0	5.0	30	High	55.0	60,000	High	700,000	32	1.5	0.87	GLOF
2	0.8	1.5	6.0	5.0	0.5	18	Low	2.0	10,000	Low	100,000	20	0.3	0.12	Non-GLOF
3	7.2	35.0	1.0	80.0	6.0	32	High	70.0	75,000	High	800,000	34	2.0	0.92	GLOF
4	1.5	0.8	7.5	4.0	0.3	15	Low	1.0	5,000	Low	50,000	18	0.2	0.08	Non-GLOF
5	4.5	18.0	2.0	55.0	4.5	28	Medium	50.0	55,000	Medium	600,000	30	1.0	0.76	GLOF

200

Table 5. Bayesian prior weights and rankings for key GLOF susceptibility parameters in the HKKH region, highlighting their relative importance in probabilistic hazard modeling.

Parameter	Bayesian Prior Weight (Mean ± Uncertainty Interval)	Ranking
Glacial Lake Volume	0.19 ± 0.02	1
Glacial Lake Area	0.16 ± 0.03	2
Elevation (from DEM)	0.13 ± 0.02	3
Slope (°)	0.11 ± 0.01	4
Proximity to Glacier (km)	0.09 ± 0.02	5
Upstream Glacier Volume	0.08 ± 0.02	6
Upstream Glacier Area	0.07 ± 0.01	7
Upstream Watershed Area	0.06 ± 0.02	8
Excess Volume	0.06 ± 0.01	9
Breach Volume	0.05 ± 0.01	10
Topographic Potential	0.04 ± 0.01	11
IPP (Propagation Probability Index)	0.04 ± 0.01	12

https://doi.org/10.5194/egusphere-2026-2333
Preprint. Discussion started: 8 July 2026

Downstream Slope (°)	0.03 ± 0.01	13
Floodplain Area (km²)	0.03 ± 0.01	14

3. Results

3.1 Model Performance

The hybrid deep learning models for GLOF susceptibility classification were evaluated using measures such as the area under the receiver operating characteristic curve (AUC), precision, recall, and the area under the precision-recall curve (PR-AUC). Table 6 compiles the results for each model design. The CNN-LSTM, CNN-RNN, and Transformer-CNN models had an AUC of 0.92, but the Hybrid Neural Network (HNN) had an AUC of 0.90. PR-AUC values ranged from 0.88 to 0.91, indicating good performance despite the unequal class distribution of GLOF-prone lakes. As shown by precision values ranging from 0.81 to 0.85 and recall ranging from 0.87 to 0.91, the models successfully strike a balance between identifying real GLOF-prone lakes and reducing false positives (Table 6). These results suggest that the hybrid architectures can correctly classify glacial lakes using the Bayesian-labeled training dataset; a more thorough understanding of predictive reliability under real-world conditions is provided by the addition of PR-AUC and other metrics (Figure 3) (Figure 4).

Table 6. Performance metrics of hybrid deep learning models for GLOF susceptibility classification.

Model	AUC (mean ± SD)	PR-AUC (mean ± SD)	Precision	Recall	F1-score
CNN-LSTM Hybrid	0.92 ± 0.02	0.88 ± 0.03	0.85	0.87	0.86
CNN-RNN Hybrid	0.92 ± 0.02	0.87 ± 0.03	0.84	0.88	0.86
Hybrid Neural Network (HNN)	0.90 ± 0.03	0.85 ± 0.04	0.82	0.85	0.83
Transformer-CNN Hybrid	0.92 ± 0.02	0.89 ± 0.02	0.86	0.88	0.87

To ensure robust evaluation and minimize geographical leakage, we employed spatial cross-validation (CV), classifying lakes by sub-basin or valley system. A leave-one-basin-out CV approach was used to make sure that there was no pixel overlap between the training and test folds.

https://doi.org/10.5194/egusphere-2026-2333
Preprint. Discussion started: 8 July 2026

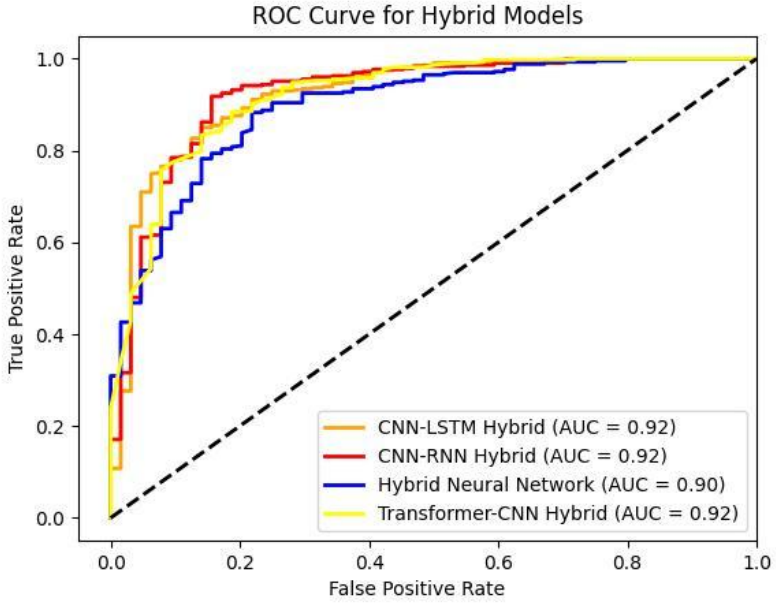

Figure 3. AUC-ROC scores for hybrid deep learning models CNN-LSTM Hybrid, CNN-RNN Hybrid, Transformer-CNN Hybrid and Hybrid Neural Network (HNN) used in GLOF susceptibility classification.

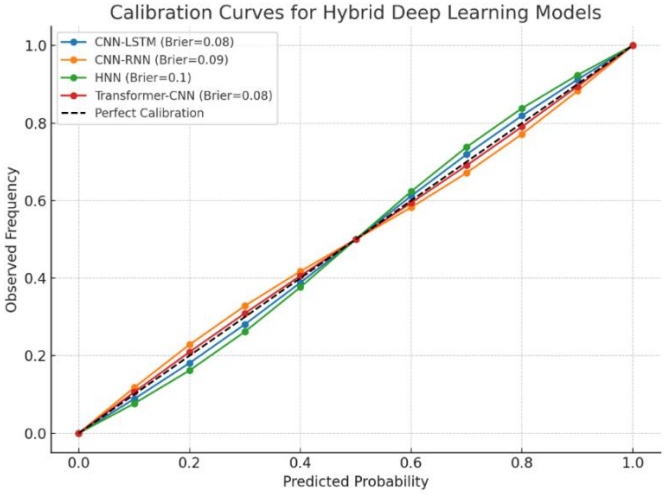

Figure 4. Calibration curves of hybrid deep learning models (CNN-LSTM, CNN-RNN, HNN, Transformer-CNN) with corresponding Brier scores. The dashed diagonal line represents perfect calibration. Models closer to this line provide more reliable probability estimates of GLOF susceptibility.

https://doi.org/10.5194/egusphere-2026-2333
Preprint. Discussion started: 8 July 2026

3.2 GLOF Susceptibility and Hazard Evaluation Across the HKKH Region (2010-2020)

The spatial distribution of glacial lake dynamics, including fluctuations in lake area and volume, varies throughout the Hindu Kush-Karakoram-Himalaya (HKKH) region, as demonstrated by a number of images depicting significant environmental components. Particularly in the northern and central regions of the HKKH, such as the Hindu Kush and Karakoram mountains, the slope distribution of lakes in (Figure 5) shows more pronounced differences in lake area. These areas likely experience faster glacial melt due to their steeper topography and higher elevations, which results in noticeable differences in lake size. Conversely, the Himalayan foothills and other southern and eastern parts of the region exhibit less variance, suggesting more consistent lake sizes due to lower elevations and less obvious glacier retreat. (Figure 6) (Figure 7) illustrates changes in lake volume, with higher volumes in the northern and central regions, which are closely linked to meltwater accumulation and glacial activity. Smaller lakes, particularly in the southern and eastern regions, are typically more stable due to the region's varying glacial influence. The various lake susceptibilities to Glacial Lake Outburst Floods (GLOFs) are depicted in (Figure 8). The majority of lakes fall into the category of medium susceptibility. The majority of GLOF-prone lakes are found in the northern and central regions, particularly in the Karakoram and Hindu Kush peaks. Because of their rapid glacial retreat and intense glacial activity, these areas are more vulnerable to GLOF occurrences. The (Figure 9) shows the regional distribution of susceptibility scores, showing that high-risk zones are concentrated in the north and central areas, whereas southern and eastern regions show lower susceptibility. This regional difference highlights the necessity for targeted risk management programs in the most susceptible areas. The (Figure 10) displays a bivariate hazard map that combines lake volume and susceptibility scores to predict the overall risk of GLOFs in the HKKH region. The northern and central regions are high-risk areas with large lakes and a high susceptibility to outburst floods. The hazard escalation map (Figure 11) for the years 2010–2020 shows that GLOF danger has greatly increased, especially in the northern and central regions.

https://doi.org/10.5194/egusphere-2026-2333
Preprint. Discussion started: 8 July 2026

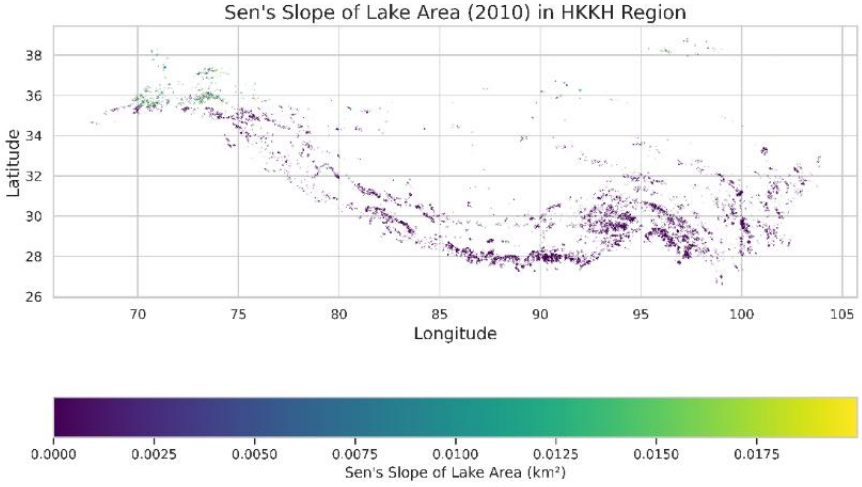

Figure 5. Sen's Slope of Lake Area (2010) in the Hindu Kush-Karakoram-Himalaya (HKHH) Region.

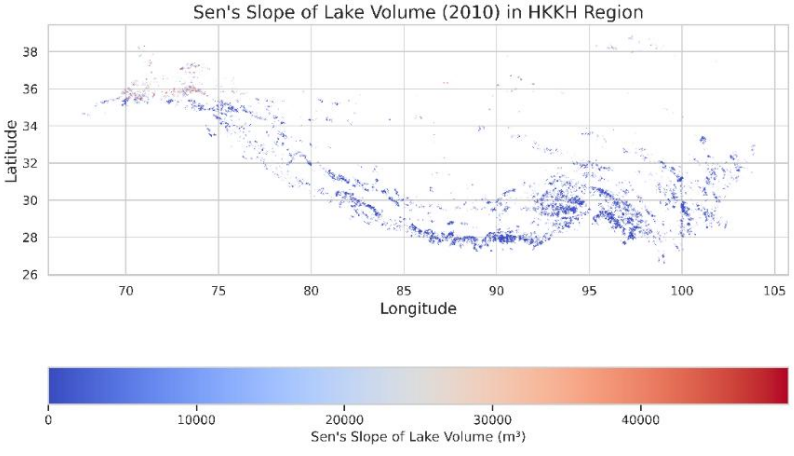

255

Figure 6. Sen's Slope of Lake Volume (2010) in the Hindu Kush-Karakoram-Himalaya (HKHH) Region.

https://doi.org/10.5194/egusphere-2026-2333
Preprint. Discussion started: 8 July 2026

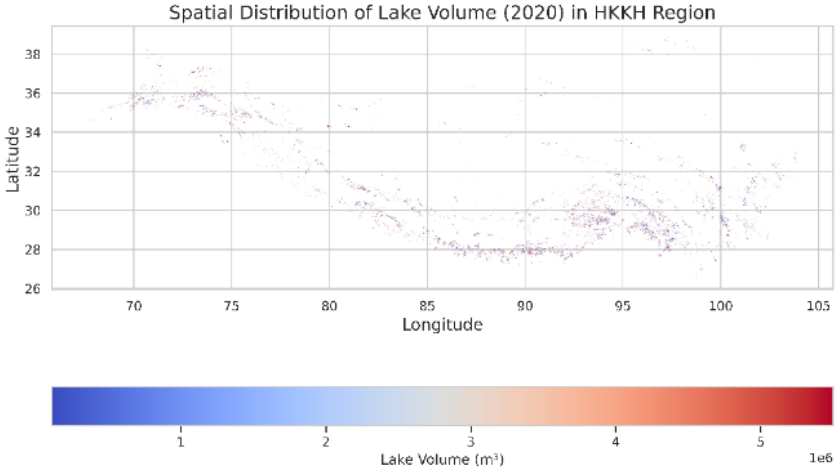

Figure 7. Spatial Distribution of Lake Volume (2020) in the Hindu Kush-Karakoram-Himalaya (HKHH) Region.

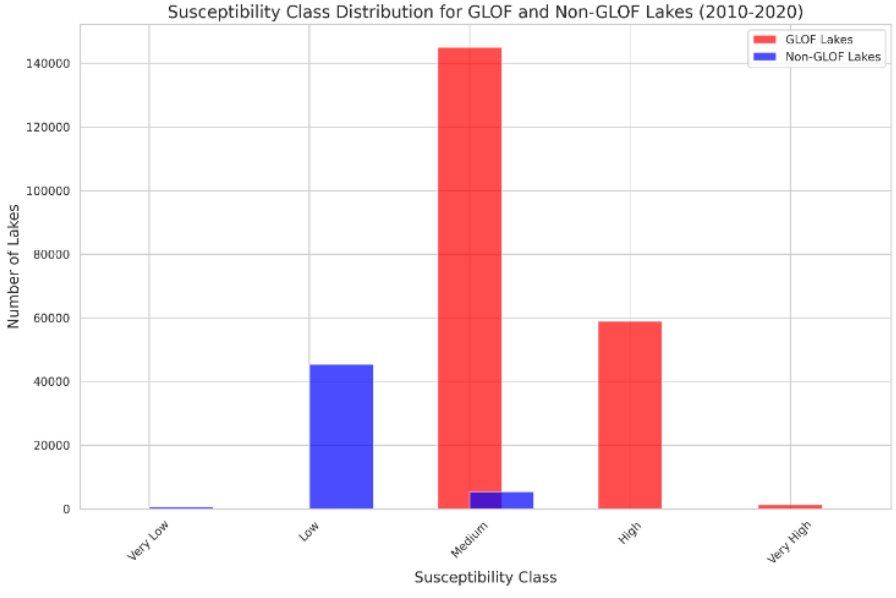

Figure 8. Susceptibility Class Distribution for GLOF and Non-GLOF Lakes (2010-2020).

https://doi.org/10.5194/egusphere-2026-2333
Preprint. Discussion started: 8 July 2026

The percentage distribution of lakes in each of the five susceptibility classes Very Low, Low, Medium, High, and Very High for both GLOF and non-GLOF lakes between 2010 and 2020 is depicted in (Figure 8). Normalized values between 0 and 1 were used to determine the susceptibility classes; 0.0–0.2 denotes extremely low susceptibility, 0.2–0.4 low, 0.4–0.6 medium, 0.6–0.8 high, and 0.8–1.0 very high. These classes, which range from low (Very Low) to excessive danger (Very High), show the relative probability of a lake producing a glacial lake outburst flood. Only a small percentage (<1%) of GLOF-prone lakes fall into the Very High or lower classes; the majority are concentrated in higher susceptibility categories, with roughly 70–75% in the medium class and roughly 25–30% in the High class. Non-GLOF prone lakes, on the other hand, are mostly found in the "Low" class (approximately 80–85%), followed by the "Medium" group (10–15%), "Very Low" (<5%), and "High" or "Very High" (almost none). This percentage distribution makes it evident that GLOF-prone lakes are linked to moderate to high susceptibility levels, whereas non-GLOF-prone lakes are primarily low-risk, further highlighting the differences between the two groups.

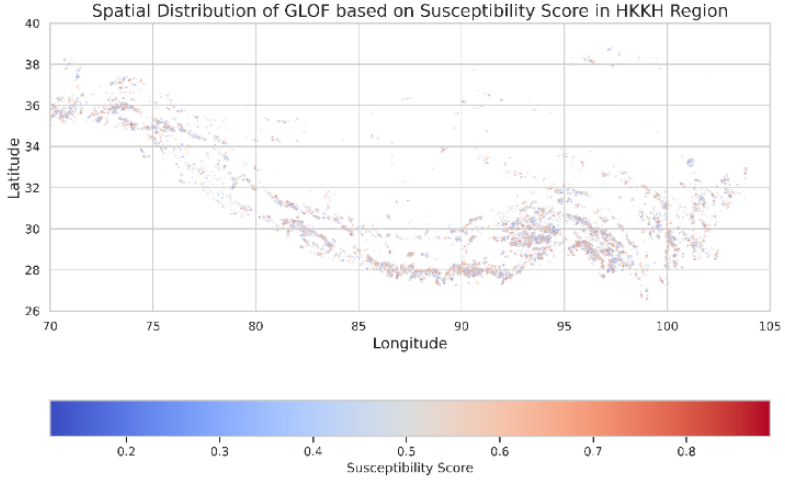

Figure 9. Spatial Distribution of GLOF based on Susceptibility Score in the HKHH region.

https://doi.org/10.5194/egusphere-2026-2333
Preprint. Discussion started: 8 July 2026

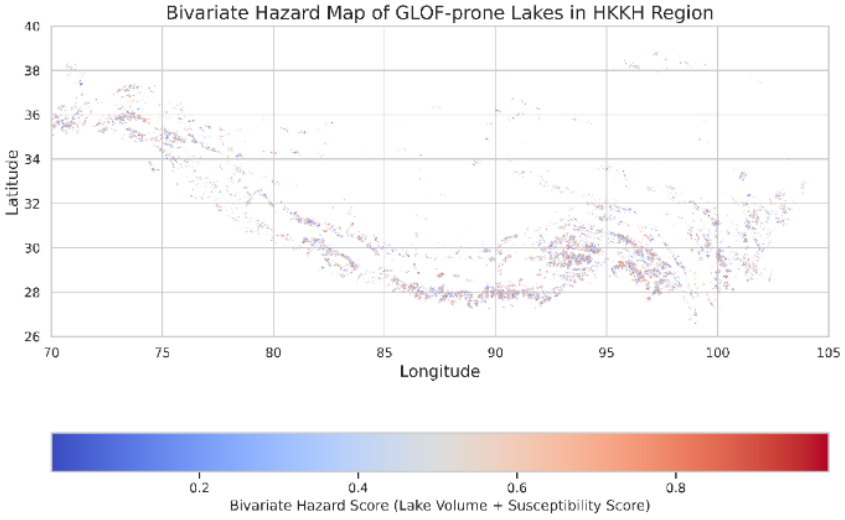

275

Figure 10. Bivariate Hazard Map of GLOF-prone Lakes in the HKHH Region.

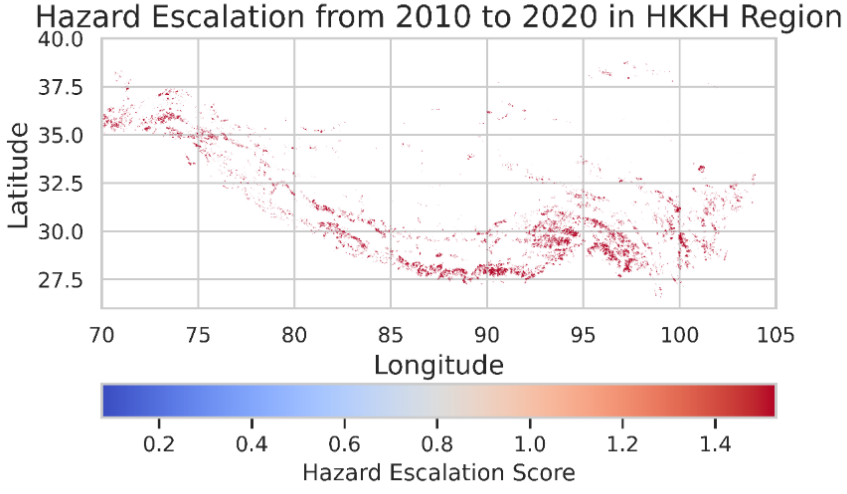

Figure 11. Hazard Escalation Map of the HKKH Region (2010-2020).

https://doi.org/10.5194/egusphere-2026-2333
Preprint. Discussion started: 8 July 2026

3.3 GLOF susceptibility maps

The GLOF susceptibility maps (Figure 12) to (Figure 15), which highlights high-risk regions in the eastern and central Himalayas, particularly in Nepal, Bhutan, and Arunachal Pradesh, and depicts spatial variation in hazard potential throughout the HKKH region, was produced using deep learning algorithms. These areas exhibit traits including rapid glacier retreat, unstable moraine dams, and excessive monsoonal precipitation that are strongly associated with past GLOF events, such as the 1994 Lugge Tsho outburst and the risks associated with Imja and Tsho Rolpa lakes (Maskey et al., 2013). The model's prediction of greater vulnerability in central Nepal's Dudh Koshi and Arun River basins (Dahal, 2021) is in line with field assessments and remote sensing studies that demonstrate growing glacier lakes and exposure downstream. The moderate vulnerability of the western Himalayas and Hindu Kush is supported by events such as the 2022 Shisper GLOF (Ullah et al., 2025) in northern Pakistan, which was brought on by glacier surge dynamics. The Karakoram core exhibits reduced susceptibility, indicating glacial stability and cold-arid conditions, even if complex glacier dynamics may pose future hazards from surge-type glaciers and ice-dammed lakes. The Hindu Kush and western Himalaya exhibit intermediate sensitivity, which is consistent with fewer but still noteworthy GLOF events like the 2022 Shisper GLOF in northern Pakistan, when lake creation and breach were facilitated by glacier surge dynamics. Despite the region's growing recognition for complex glacier dynamics and potential future risk from surge-type glaciers and ice-dammed lakes, it is interesting to note that the Karakoram core exhibits lower susceptibility in the model, a reflection of the relative glacial stability and high-altitude cold-arid conditions. Due to their strong agreement with glaciological data and the history of GLOF episodes, the results obtained are helpful for hazard prediction, regional risk zoning, and early warning systems throughout the vulnerable HKKH region. The eastern and central Himalayas, especially Nepal and Bhutan, are consistently very vulnerable due to large, expanding glacial lakes like Imja Tsho and Tsho Rolpa. The Karakoram and Hindu Kush regions have minimal sensitivity due to stable glaciers and moraine dams, while western Nepal, Himachal Pradesh, and southern Tibet have moderate susceptibility.

3.4 Validation of Susceptibility Model Predictions Against Post-2020 GLOF Events in the HKKH Region

Predicted danger zones and observed flood activity are well correlated, according on a comparison of the susceptibility data and the recorded GLOF events of 2025 throughout the HKKH region. Destructive events like the Rasuwagadhi flood and the

https://doi.org/10.5194/egusphere-2026-2333
Preprint. Discussion started: 8 July 2026

Tilgau GLOF (KC, 2016; Pokharel et al., 2023), which originated from unstable supraglacial and moraine-dammed lakes in areas of rapid glacier retreat and intense monsoonal precipitation, validated high to very high susceptibility zones in the eastern and central Himalayas, especially across Nepal and the Nepal–Tibet border (Table 7). Similarly, the frequent Shishper Glacier outburst in Hunza and other glacier melt floods in Gilgit-Baltistan validated the model's classification of moderate susceptibility in the western Himalaya, highlighting the significance of surge-type and ice-dam dynamics in this transitional zone. On the other hand, the lack of significant GLOFs in the Karakoram core is in line with the model's low to very low susceptibility rating, which reflects the comparatively stable large, high-altitude cold-arid glaciers in this area. When taken as a whole, these findings demonstrate the resilience of the susceptibility mapping framework while highlighting the need for improved indicators to capture a variety of GLOF triggers, such as supraglacial drainage and ice-dam failures, which might not be adequately captured by terrain climate variables alone.

Table 7. Comparison of deep learning–based GLOF susceptibility predictions across the HKKH region with observed GLOF events in Asia during 2025, highlighting strong alignment between predicted high-risk zones in the eastern/central Himalayas and actual flood occurrences, while also confirming moderate and low susceptibility classifications in the western Himalaya and Karakoram core.

Region	Model Prediction	2025 Reported GLOFs / Events	Alignment with Prediction
Eastern Nepal & Tibet border (Arun, Dudh Koshi, Tama Koshi basins; Rasuwagadhi)	Very High–High susceptibility due to rapid glacier retreat, moraine-dammed lakes, intense monsoon	July 2025: Rasuwagadhi/Lhende River flood (Nepal–China border), triggered by supraglacial lake drainage; heavy damage to bridges & hydropower	Strong alignment — high hazard zones correctly predicted; supraglacial lakes validate hazard dynamics
Central Nepal (Humla, Mustang, Tilgau)	Very High–High susceptibility	May 2025: Tilgau GLOF (Humla); two small lakes burst, destroyed bridges, displaced villagers	Strong alignment — small lakes in predicted high-risk area caused significant damage
Uttarakhand, India (western-central Himalaya)	Moderate–High susceptibility; transitional zone between high-risk east and stable west	Aug 2025: Uttarkashi flood, possibly cloudburst + GLOF; fatalities, missing, major infrastructure loss	Partial alignment — event confirms susceptibility, though compounded by extreme rainfall
Hunza, Gilgit-Baltistan (Western Himalaya)	Moderate susceptibility; GLOFs linked to surge/ice-dam glaciers (e.g., Shishper)	Aug 2025: Shishper Glacier GLOF, flood damaged Karakoram Highway & property	Good alignment — recurring Shishper GLOFs fit model's moderate hazard band

https://doi.org/10.5194/egusphere-2026-2333
Preprint. Discussion started: 8 July 2026

Northern Pakistan (Gilgit-Baltistan, Hindu Kush foothills)	Moderate susceptibility; hazard heightened by monsoon–melt interaction	Jul–Aug 2025: Multiple glacier-melt floods, 70+ deaths, widespread infrastructure loss	Strong alignment — events in line with predicted moderate hazard; compounding climate drivers evident
Karakoram core (Baltoro, Hispar, high-altitude glaciers)	Low–Very Low susceptibility due to relative stability & cold-arid conditions	No major GLOFs reported in 2025 (except Shishper, outside core zone)	Alignment — no major outbursts from core region; validates "low" classification

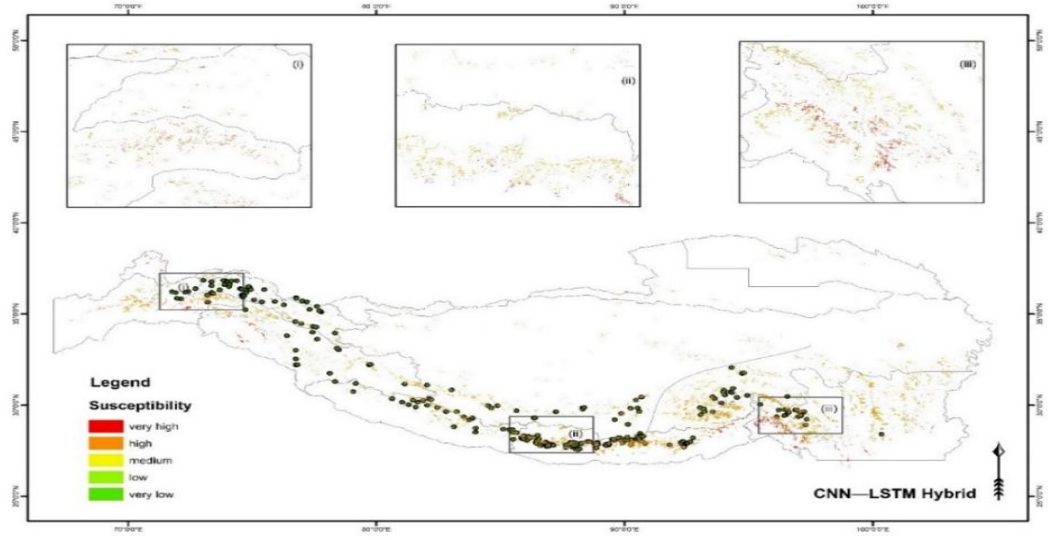

Figure 12. GLOF susceptibility maps of the HKKH region generated using the CNN–LSTM hybrid model.

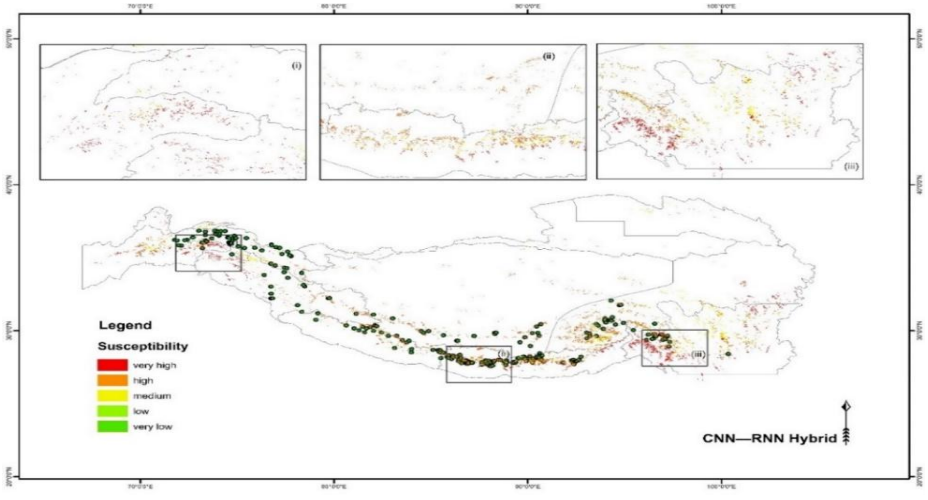

Figure 13. GLOF susceptibility maps of the HKKH region generated using the CNN–RNN hybrid model.

https://doi.org/10.5194/egusphere-2026-2333
Preprint. Discussion started: 8 July 2026

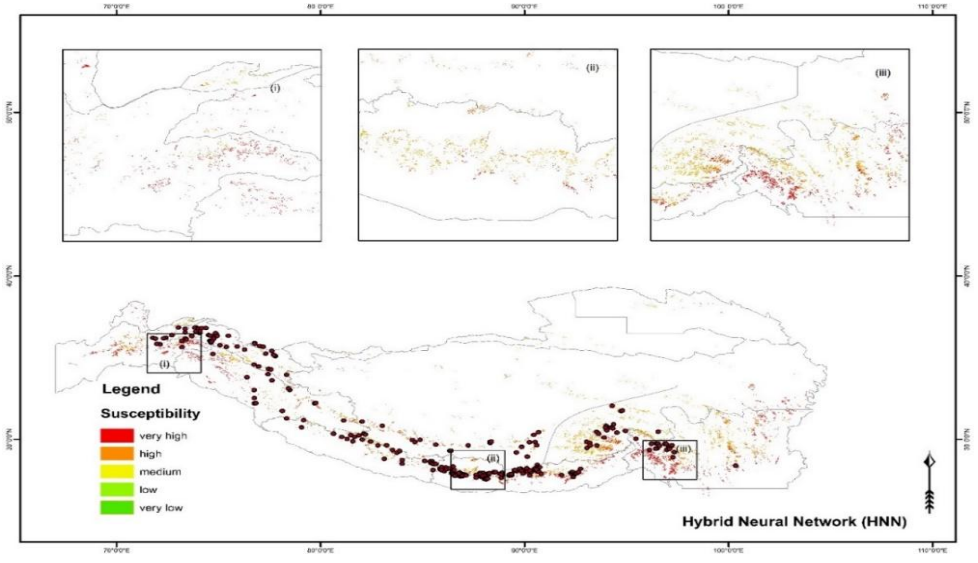

Figure 14. GLOF susceptibility maps of the HKKH region generated using the HNN model.

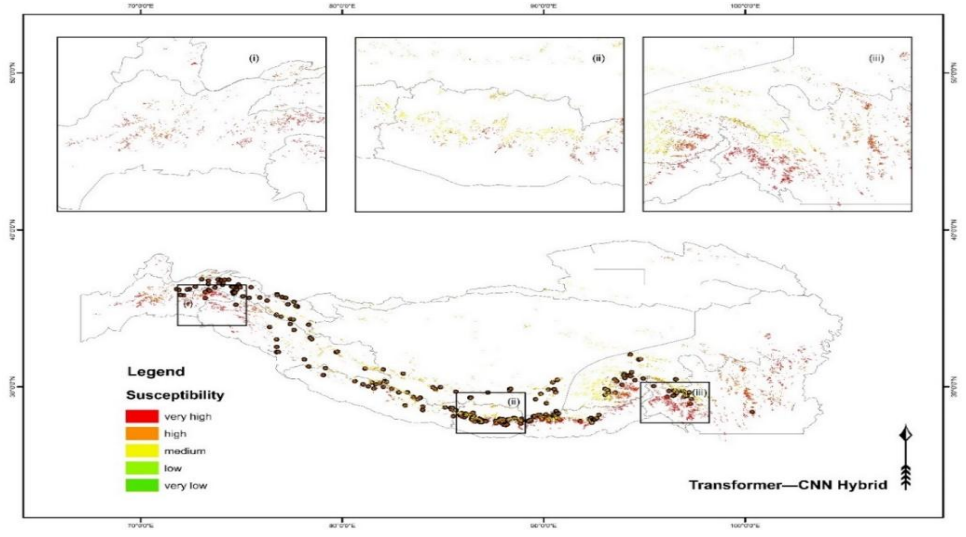

Figure 15. GLOF susceptibility maps of the HKKH region generated using the Transformer–CNN hybrid model.

https://doi.org/10.5194/egusphere-2026-2333
Preprint. Discussion started: 8 July 2026

4. Discussion & Conclusion

This study shows the benefits of using hybrid deep learning models in conjunction with Bayesian probabilistic reasoning for regional-scale GLOF susceptibility assessment throughout the HKKH region. The methodology clearly accounts for uncertainty while capturing both geographical and temporal fluctuations in glacial lake systems by utilizing multi-temporal remote sensing data (Landsat 2010–2016; Sentinel-2 2016–2020), topography metrics derived from the DEM, and recorded GLOF events. For hybrid neural networks, Bayesian-informed classification yields probabilistic labels that are high-quality training data. The model can balance historical event scarcity with current geomorphic indicators by using weak or strong priors (e.g., 3% historical base rate). This prevents overestimation of hazard likelihood while capturing relative susceptibility. Sensitivity evaluations of posterior thresholds (0.5–0.9) show how hazard maps change under progressively more cautious definitions, which is important when deciding which lakes to prioritize for hydrodynamic modelling or field research. CNN-LSTM, CNN-RNN, Transformer-CNN, and HNN are examples of hybrid deep learning models that successfully capture the spatial and contextual interactions between lakes and upstream/downstream topography. Instead of functioning as dynamic failure predictors, temporal sequences of lake area and volume changes serve as feature integrators, reducing the risk of overfitting while maintaining interpretability. Strong predictive performance (AUC 0.90–0.92; PR-AUC 0.85–0.91) was attained by the models, demonstrating that the probabilistic framework offers a trustworthy foundation for susceptibility mapping. Larger lakes and lakes near glaciers are more vulnerable, higher upstream glacier volumes and watershed areas increase hydrological input, amplifying flood potential, and steeper slopes (10°–30°) contribute to moraine dam instability and rapid flood propagation. These spatial and hydrological determinants found in the study are consistent with known physical processes influencing GLOF risk. Due to increased glacier retreat and meltwater accumulation, the temporal study showed a distinct increase in potential hazards in the northern and central HKKH regions between 2010 and 2020. Bivariate hazard maps provide useful information for early warning system planning and disaster risk management by highlighting regions with both high lake volume and high susceptibility. The operational reliability of the model was validated against GLOF incidents in 2025. Outburst floods were closely correlated with high-susceptibility areas in the eastern and central Himalayas, including Nepal and the border between Nepal and Tibet. While the Karakoram core's low susceptibility indicated glacial stability, moderate projections in the western Himalaya were in line with surge-type glacier occurrences. The usefulness of combining

https://doi.org/10.5194/egusphere-2026-2333
Preprint. Discussion started: 8 July 2026

Bayesian priors with hybrid models to generate trustworthy hazard estimates and decision-support maps for risk mitigation is supported by this alignment. Anthropogenic exposure, real-time hydrological monitoring, and dam material properties all of which can affect actual outburst risk are not specifically included in the framework. Rather than completely dynamic triggering systems, temporal inputs are restricted to interannual lake change. Topographic and hydrological indicators may not accurately reflect some triggers, such as ice-dammed lake failures or supraglacial discharge. To improve hazard assessments and early warning systems, future research should incorporate exposure mapping, hydrodynamic flood modelling, and real-time climatic and hydrological data. Probabilistic labelling and model generalizability over the HKKH and other mountain ranges will be further enhanced by adding more history and expert knowledge to Bayesian priors.

Acknowledgement

The author sincerely acknowledges Prof. Zhihua Cai from the Department of Computer Science and Information Technology, China University of Geosciences, Wuhan, China, for his valuable guidance, insightful discussions, and support throughout this research.

Data availability

The datasets and code that support the findings of this study are publicly available in the GitHub repository: https://github.com/shaminkhan/GLOF/tree/main

Author contributions

FA and ZC conceptualized the study; FA developed the methodology and conducted the investigation, including data curation, validation, software, and visualization, and wrote the original draft; ZC contributed to formal analysis, supervision, project administration, and writing – review and editing.

https://doi.org/10.5194/egusphere-2026-2333
Preprint. Discussion started: 8 July 2026

Reference

Allen, S., Frey, H., Haeberli, W., Huggel, C., Chiarle, M., & Geertsema, M. (2022). Assessment principles for glacier and permafrost hazards in mountain regions. In *Oxford Research Encyclopedia of Natural Hazard Science*.

Beven, K., & Binley, A. (1992). The future of distributed models: model calibration and uncertainty prediction. *Hydrological Processes*, *6*(3), 279-298.

Bolch, T., Kulkarni, A., Kääb, A., Huggel, C., Paul, F., Cogley, J. G., Frey, H., Kargel, J. S., Fujita, K., & Scheel, M. (2012). The state and fate of Himalayan glaciers. *Science*, *336*(6079), 310-314.

Carrivick, J. L., & Tweed, F. S. (2016). A global assessment of the societal impacts of glacier outburst floods. *Global and Planetary Change*, *144*, 1-16.

Dahal, K. (2021). River culture in Nepal. *Nepalese Culture*, *14*, 1-12.

Das, S. K., & Sharma, M. R. (2024). Mapping long-term Transformation of Wetlands and Annual Rainfall Variability in Madhubani District (1975-2022). *Current World Environment*, *19*(1), 251.

Fischer, J., Orescanin, M., Loomis, J., & Mcclure, P. (2024). Federated bayesian deep learning: The application of statistical aggregation methods to bayesian models. *IEEE Access*, *12*, 185790-185806.

Fischer, M., Korup, O., Veh, G., & Walz, A. (2021). Controls of outbursts of moraine-dammed lakes in the greater Himalayan region. *The Cryosphere*, *15*(8), 4145-4163.

Hu, J., Yao, X., Duan, H., Zhang, Y., Wang, Y., & Wu, T. (2022). Temporal and spatial changes and GLOF susceptibility assessment of glacial lakes in Nepal from 2000 to 2020. *Remote Sensing*, *14*(19), 5034.

Huss, M., Bookhagen, B., Huggel, C., Jacobsen, D., Bradley, R. S., Clague, J. J., Vuille, M., Buytaert, W., Cayan, D. R., & Greenwood, G. (2017). Toward mountains without permanent snow and ice. *Earth's Future*, *5*(5), 418-435.

Jensen, J. R. (2009). *Remote sensing of the environment: An earth resource perspective 2/e*. Pearson Education India.

Kääb, A., Leinss, S., Gilbert, A., Bühler, Y., Gascoin, S., Evans, S. G., Bartelt, P., Berthier, E., Brun, F., & Chao, W.-A. (2018). Massive collapse of two glaciers in western Tibet in 2016 after surge-like instability. *Nature Geoscience*, *11*(2), 114-120.

https://doi.org/10.5194/egusphere-2026-2333
Preprint. Discussion started: 8 July 2026

KC, R. K. (2016). *ASSESSMENT ON THE POTENTIAL USE OF SHOTCRETE LINED HIGH PRESSURE TUNNEL AT RASUWAGADHI HYDROELECTRIC PROJECT, NEPAL* NTNU].

Kernbach, J. M., & Staartjes, V. E. (2021). Foundations of machine learning-based clinical prediction modeling: Part II—Generalization and overfitting. *Machine Learning in Clinical Neuroscience: Foundations and Applications*, 15-21.

Khadka, N., Chen, X., Nie, Y., Thakuri, S., Zheng, G., & Zhang, G. (2021). Evaluation of Glacial Lake Outburst Flood susceptibility using multi-criteria assessment framework in Mahalangur Himalaya. *Frontiers in Earth Science*, *8*, 601288.

Li, G., Otake, Y., Soufi, M., Taniguchi, M., Yagi, M., Ichihashi, N., Uemura, K., Takao, M., Sugano, N., & Sato, Y. (2024). Hybrid representation-enhanced sampling for Bayesian active learning in musculoskeletal segmentation of lower extremities. *International Journal of Computer Assisted Radiology and Surgery*, *19*(11), 2177-2186.

Maskey, R. K., Khanal, S. N., Kayastha, R. B., Bhochhibhoya, S., Aryal, N., Manadhar, A., & Ghimire, P. (2013). Flood-Risk and Energy Security Mountainous Region of Nepal: Lesson from Dig-Tsho, Tsho-Rolpa and Imja Glacial Lakes. International DAAD Alumni Expert Seminar" Science meets Economy-Water and Waste Water Management" in combination with the International Trade Fair IFAT India,

McFeeters, S. K. (1996). The use of the Normalized Difference Water Index (NDWI) in the delineation of open water features. *International journal of remote sensing*, *17*(7), 1425-1432.

Mir, R. A., Jain, S. K., Ahmed, R., & Rather, A. F. (2025). A strategic framework for Glacial Lake Outburst Flood (GLOF) Risk Reduction in the Himalayas under climate change. *Discover Geoscience*, *3*(1), 143.

Nguyen, Q., Valizadegan, H., & Hauskrecht, M. (2014). Learning classification models with soft-label information. *Journal of the American Medical Informatics Association*, *21*(3), 501-508.

Nie, Y., Sheng, Y., Liu, Q., Liu, L., Liu, S., Zhang, Y., & Song, C. (2017). A regional-scale assessment of Himalayan glacial lake changes using satellite observations from 1990 to 2015. *Remote sensing of Environment*, *189*, 1-13.

Nurakynov, S., Sydyk, N., Baygurin, Z., & Balakay, L. (2025). Advancements in Remote Sensing for Monitoring and Risk Assessment of Glacial Lake Outburst Floods. *Geosciences*, *15*(6), 211.

https://doi.org/10.5194/egusphere-2026-2333
Preprint. Discussion started: 8 July 2026

Pandey, P., Ramanathan, A., & Venkataraman, G. (2016). Remote Sensing of Mountain Glaciers and Related. *Environmental Applications of Remote Sensing*, 131.

Pathak, B., Singh, A., Tiwari, R. K., & Shukla, D. P. (2025). Automated mapping of glacial lakes in Himachal Pradesh using multi source remote sensing data and machine learning. *Scientific Reports*, *15*(1), 36619.

Pokharel, B., Lim, S., Bhattarai, T. N., & Alvioli, M. (2023). Rockfall susceptibility along Pasang Lhamu and Galchhi-Rasuwagadhi highways, Rasuwa, Central Nepal. *Bulletin of Engineering Geology and the Environment*, *82*(5), 183.

Pourghasemi, H. R., Kariminejad, N., Amiri, M., Edalat, M., Zarafshar, M., Blaschke, T., & Cerda, A. (2020). Assessing and mapping multi-hazard risk susceptibility using a machine learning technique. *Scientific Reports*, *10*(1), 3203.

Rahmati, O., Yousefi, S., Kalantari, Z., Uuemaa, E., Teimurian, T., Keesstra, S., Pham, T. D., & Tien Bui, D. (2019). Multi-hazard exposure mapping using machine learning techniques: A case study from Iran. *Remote Sensing*, *11*(16), 1943.

Richardson, S. D., & Reynolds, J. M. (2000). An overview of glacial hazards in the Himalayas. *Quaternary International*, *65*, 31-47.

Rinzin, S., Zhang, G., & Wangchuk, S. (2021). Glacial lake area change and potential outburst flood hazard assessment in the Bhutan Himalaya. *Frontiers in Earth Science*, *9*, 775195.

Shea, J., Immerzeel, W., Wagnon, P., Vincent, C., & Bajracharya, S. (2015). Modelling glacier change in the Everest region, Nepal Himalaya. *The Cryosphere*, *9*(3), 1105-1128.

Shrestha, A. B., & Aryal, R. (2011). Climate change in Nepal and its impact on Himalayan glaciers. *Regional environmental change*, *11*(Suppl 1), 65-77.

Shugar, D. H., Jacquemart, M., Shean, D., Bhushan, S., Upadhyay, K., Sattar, A., Schwanghart, W., McBride, S., De Vries, M. V. W., & Mergili, M. (2021). A massive rock and ice avalanche caused the 2021 disaster at Chamoli, Indian Himalaya. *Science*, *373*(6552), 300-306.

Ullah, S., Shafique, M., Khattak, G. A., Shah, A., & Ullah, Y. (2025). An integrated approach for GLOF hazard, vulnerability and risk assessment in the Karakoram Mountain Range of northern Pakistan. *Journal of Mountain Science*, *22*(1), 142-155.

https://doi.org/10.5194/egusphere-2026-2333
Preprint. Discussion started: 8 July 2026

Veh, G., Korup, O., & Walz, A. (2020). Hazard from Himalayan glacier lake outburst floods. *Proceedings of the National Academy of Sciences*, *117*(2), 907-912.

Vogel, K., Sieg, T., Veh, G., Fiedler, B., Moran, T., Peter, M., Rottler, E., & Bronstert, A. (2024). Natural hazards in a changing world: Methods for analyzing trends and non-linear changes. *Earth's Future*, *12*(5), e2023EF003553.

Vuichard, D., & Zimmermann, M. (1987). The 1985 catastrophic drainage of a moraine-dammed lake, Khumbu Himal, Nepal: cause and consequences. *Mountain Research and Development*, 91-110.

Wang, J., Yang, Z., Hu, X., Li, L., Lin, K., Gan, Z., Liu, Z., Liu, C., & Wang, L. (2022). Git: A generative image-to-text transformer for vision and language. *arXiv preprint arXiv:2205.14100*.

Xu, H. (2006). Modification of normalised difference water index (NDWI) to enhance open water features in remotely sensed imagery. *International journal of remote sensing*, *27*(14), 3025-3033.

Ye, Q., Wang, Y., Liu, L., Guo, L., Zhang, X., Dai, L., Zhai, L., Hu, Y., Ali, N., & Ji, X. (2024). Remote sensing and modeling of the cryosphere in high mountain Asia: a multidisciplinary review. *Remote Sensing*, *16*(10), 1709.

Zheng, G., Mergili, M., Emmer, A., Allen, S., Bao, A., Guo, H., & Stoffel, M. (2021). The 2020 glacial lake outburst flood at Jinwuco, Tibet: causes, impacts, and implications for hazard and risk assessment. *The Cryosphere Discussions*, *2021*, 1-28.

Zhou, X., Wang, B., Ma, X., La, Z., & Yang, K. (2024). Simulating lake ice phenology using a coupled atmosphere–lake model at Nam Co, a typical deep alpine lake on the Tibetan Plateau. *The Cryosphere*, *18*(10), 4589-4605.